International Journal Software Engineering and Computer Science (IJSECS)
6 (2), 2026, 775-788
Published Online August 2026 in IJSECS (http://www.journal.lembagakita.com/index.php/ijsecs)
P-ISSN: 2776-4869, E-ISSN: 2776-3242. DOI: https://doi.org/10.35870/ijsecs.v6i2.7620.

RESEARCH ARTICLE Open Access

Optimization of Skin Disease Image Segmentation: A Hybrid Approach Using HE-LAB Color Space with Canny and Otsu Methods

Andi Saidah [1], Tundo [2*], I Made Agus Oka Gunawan [3], Roy Kasiono [4]

[1] Department of Machine Engineering, Universitas 17 Agustus 1945 Jakarta, North Jakarta City, Special Capital Region of Jakarta, Indonesia.
[2*] Department of Informatics Engineering, Universitas Pancasila, South Jakarta City, Special Capital Region of Jakarta, Indonesia.
[3] Department of Informatics Management, Politeknik Negeri Bali, Badung Regency, Bali Province, Indonesia.
[4] Department of Sea and Port Transportation, Sekolah Tinggi Ilmu Pelayaran Jakarta, North Jakarta City, Special Capital Region of Jakarta, Indonesia.

**Corresponding author*: asna8mujahid@gmail.com.

Received: June 18, 2026; Accepted: July 3, 2026; Published: August 1, 2026.

Abstract: Skin lesion detection through image analysis requires accurate segmentation methods to distinguish lesion regions from surrounding healthy skin. This study evaluates a hybrid approach that combines contrast enhancement using Histogram Equalization (HE) and HE applied to the Lightness (L) channel in the LAB color space (HE+LAB) with two segmentation methods, namely Canny edge detection and Otsu thresholding. The segmentation performance was evaluated at three image resolutions: 64 × 64, 128 × 128, and 256 × 256 pixels, using Accuracy, Precision, Recall, F1-Score, and Intersection over Union (IoU). The experimental results show that the HE+LAB-Otsu combination consistently achieves higher performance than the other evaluated combinations across the three resolutions. At 128 × 128 pixels, HE+LAB-Otsu achieves an Accuracy of 0.7170, F1-Score of 0.7407, and IoU of 0.5882. Canny-based segmentation generally produces lower scores, particularly for Recall and IoU, indicating difficulties in extracting complete lesion regions. The use of HE in the LAB color space improves lesion contrast while preserving the chromatic components of the image, resulting in better segmentation performance than standard HE in the evaluated experiments. The results indicate that the combination of HE+LAB and Otsu thresholding is a promising conventional approach for skin lesion image segmentation. However, further evaluation using additional datasets, statistical testing, and comparisons with modern deep learning segmentation methods is required to assess its generalizability and applicability to automated dermatological image analysis.

Keywords: HE-LAB Color Space; Hybrid Approach; Otsu Thresholding; Canny Edge Detection; Skin Lesion Image Segmentation.

1. Introduction

Skin diseases represent a significant public health concern and affect individuals across different age groups and populations. These conditions include melanoma, psoriasis, dermatitis, and various bacterial or fungal infections, ranging from relatively mild conditions to diseases that may cause serious complications when left undiagnosed or untreated. Early detection and accurate diagnosis are particularly important for serious conditions such as melanoma, for which the stage of detection is closely associated with patient outcomes. In clinical practice, skin lesions are commonly examined using dermoscopic images and visual assessment by dermatologists. Although these approaches remain important in clinical diagnosis, the interpretation of lesion characteristics can be affected by differences in lesion appearance and observer assessment. These limitations have encouraged the development of computer-aided methods that can assist the analysis of skin lesion images and provide more consistent image-based information.

Computer-aided diagnosis (CAD) systems based on digital image processing have been developed to support the analysis of skin lesions. Within these systems, image segmentation is an important step because it separates the lesion region from the surrounding skin and provides a basis for subsequent feature extraction, classification, and analysis. However, accurate skin lesion segmentation remains challenging because lesions may vary considerably in shape, size, color, and boundary characteristics. Image acquisition conditions can further introduce artifacts such as hair, shadows, noise, and uneven illumination, making it difficult to distinguish lesion regions from healthy skin. These conditions can affect the quality of the segmentation result and may lead to incomplete or inaccurate lesion boundaries. Therefore, appropriate preprocessing techniques are required to improve image contrast and make lesion regions more distinguishable before the segmentation process.

Histogram Equalization (HE) is a conventional contrast enhancement technique that modifies the distribution of image intensity values to improve overall contrast. However, applying HE directly to RGB images may alter the relationships between color channels and produce unwanted color changes. An alternative is to perform contrast enhancement in a color space that separates lightness from chromatic information, such as the CIELAB color space. In this representation, the L channel describes lightness, while the a and b channels represent chromatic components. Applying HE to the L channel can enhance image contrast while reducing direct modification of the chromatic components. Previous studies have investigated histogram-based enhancement, LAB color representations, and classical segmentation methods for different image analysis tasks. However, the findings reported in these studies do not directly establish which combination of HE-based preprocessing and segmentation method is most appropriate for skin lesion segmentation under different image resolutions. In particular, a direct comparison between conventional HE and HE applied to the LAB lightness channel, combined with Canny edge detection and Otsu thresholding, remains relevant for evaluating the effect of preprocessing and segmentation choices on lesion extraction.

Based on this gap, this study evaluates a hybrid skin lesion segmentation approach that combines two contrast enhancement configurations, namely Histogram Equalization (HE) and HE applied to the Lightness channel in the LAB color space (HE+LAB), with two segmentation methods, Canny edge detection and Otsu thresholding. The experiments are conducted using three image resolutions, 64 × 64, 128 × 128, and 256 × 256 pixels, to examine how image resolution affects segmentation performance. The resulting segmentation masks are evaluated against manually annotated ground-truth masks using Accuracy, Precision, Recall, F1-Score, and Intersection over Union (IoU). Through this comparison, the study aims to identify the preprocessing and segmentation combination that provides the most consistent segmentation performance across the evaluated resolutions. The results are expected to provide a baseline for the application of conventional image processing techniques in skin lesion segmentation and for further development of computer-aided skin lesion analysis systems.

2. Related Work

Automatic skin lesion segmentation has become an important research topic in medical image analysis because accurate lesion extraction provides an important basis for subsequent computer-aided diagnosis (CAD) tasks. Various segmentation approaches have been investigated, ranging from conventional image processing techniques to deep learning-based methods. Although deep learning methods have shown strong performance in medical image segmentation, conventional image processing methods remain relevant because of their relatively simple implementation and lower methodological complexity, particularly when computational resources and implementation simplicity are considered. Based on the studies reviewed in this research, several gaps can be identified. First, the application of conventional Histogram Equalization (HE) directly to RGB images may alter color information and affect the visual characteristics of skin lesions. Second, although the LAB color space separates lightness from chromatic components, the combination of HE applied to the L channel with conventional segmentation methods has received less attention in the reviewed studies. Third, relatively few of the reviewed studies directly compare Otsu thresholding and Canny edge detection within the same preprocessing framework. Finally, the effect of image resolution on segmentation performance is not commonly evaluated together with multiple quantitative metrics, such as Accuracy, Precision, Recall, F1-Score, and Intersection over Union (IoU). To address these gaps, this study evaluates a hybrid segmentation approach that combines two contrast enhancement configurations, namely Histogram Equalization (HE) and HE applied to the L channel of the LAB color space (HE+LAB), with Otsu thresholding and Canny edge detection. The evaluation is conducted at three image resolutions, 64 × 64, 128 × 128, and 256 × 256 pixels. Unlike the reviewed studies that generally focus on a specific enhancement technique, color representation, or segmentation method, this study provides a systematic comparison of the selected preprocessing and segmentation combinations across multiple resolutions. The segmentation results are evaluated using Accuracy, Precision, Recall, F1-Score, and IoU to identify the configuration that provides the most favorable segmentation performance under the experimental conditions. The differences between the reviewed studies and the present study are summarized in Table 1.

Table 1. Comparison of Previous Studies Related to Skin Lesion Image Segmentation

Authors	Image Enhancement	Color Space	Segmentation Method	Resolution Analysis	Main Limitation
Agrawal & Desai (2024)	Not Applied	Grayscale	Canny Edge Detection	No	Focuses on reviewing the Canny algorithm without evaluating skin lesion segmentation or comparing it with region-based segmentation methods.
Al-Hatab *et al.* (2024)	Luminosity Enhancement	CIE LAB	Color-Based Segmentation	No	Uses LAB color analysis for lesion detection but does not integrate Histogram Equalization or compare different segmentation algorithms.
Ding *et al.* (2020)	Three Adaptive Sub-Histograms Equalization (TASHE)	RGB	Not Applicable (Image Enhancement Only)	No	Evaluates image enhancement without investigating its effect on skin lesion segmentation performance.
Basha *et al.* (2025)	Otsu Thresholding	Grayscale	Canny + Hough Transform	No	Focuses on lane detection rather than medical image segmentation and does not evaluate skin lesion images.
Ebele *et al.* (2025)	Not Applied	Grayscale	Sobel, Prewitt, and Canny	No	Compares edge detection algorithms without incorporating preprocessing techniques or threshold-based segmentation such as Otsu.
This study	HE and HE+LAB	LAB	Otsu Thresholding and Canny Edge Detection	Yes (64 × 64, 128 × 128, and 256 × 256)	Systematically compares HE and HE+LAB combined with Otsu and Canny across multiple image resolutions using Accuracy, Precision, Recall, F1-Score, and IoU.

3. Methodology

This study evaluates the effect of two contrast enhancement configurations, namely Histogram Equalization (HE) and HE applied to the Lightness (L) channel in the LAB color space (HE+LAB), on skin lesion segmentation performance using Canny edge detection and Otsu thresholding. The two segmentation methods are applied to the enhanced images to examine how contrast enhancement affects the resulting segmentation masks. The experiments are conducted at three image resolutions to evaluate the effect of image resolution on segmentation performance. The overall research workflow, from image preprocessing to segmentation and quantitative evaluation, is presented in Figure 1.

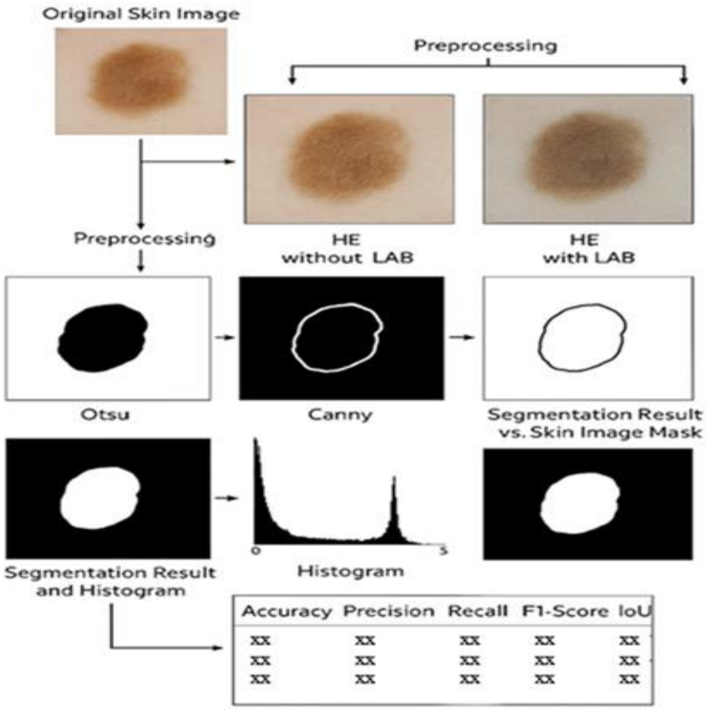

Figure 1. Research workflow.

3.1 Skin Lesion Dataset

This study uses the PH2 Dataset, a publicly available dermoscopic image dataset for skin lesion analysis. The dataset contains 200 dermoscopic images comprising common nevi, atypical nevi, and melanoma lesions. Each image is accompanied by an expert-annotated ground truth mask that identifies the lesion region, allowing quantitative evaluation of the segmentation results. To evaluate the effect of image resolution, the images are resized to three resolutions: 64 × 64, 128 × 128, and 256 × 256 pixels. The corresponding ground truth masks are also adjusted to the same resolutions for pixel-level comparison with the segmentation outputs. The image resolutions used in the experiments are presented in Table 2.

Table 2. Skin Lesion Image Resolutions Used in the Experiments

Image	Resolution
Original image	64 × 64 pixels
Resized image	128 × 128 pixels
Resized image	256 × 256 pixels

3.2 Preprocessing

Preprocessing is the initial stage of the image processing pipeline and is performed to prepare the images for subsequent segmentation. In this study, two contrast enhancement configurations are evaluated. The first configuration applies Histogram Equalization (HE) without LAB-based processing, while the second configuration converts the image to the LAB color space and applies HE to the Lightness (L) channel, referred to as HE+LAB. The enhanced images are subsequently processed using Otsu thresholding and Canny edge detection. The experimental design therefore consists of four preprocessing-segmentation combinations: HE-Otsu, HE-Canny, HE+LAB-Otsu, and HE+LAB-Canny. Each combination is evaluated at 64 × 64, 128 × 128, and 256 × 256 pixels.

3.3 Histogram Equalization (HE)

Histogram Equalization (HE) is a contrast enhancement method that redistributes pixel intensity values across the available intensity range. For an 8-bit image, the intensity range is generally 0–255. HE is particularly useful when the original image has a narrow intensity distribution, which may limit the visibility of differences between the lesion and surrounding skin. For an image with discrete intensity levels from 0 to L−1, the new intensity value sk is determined from the original intensity value tk based on the cumulative distribution of pixel intensities, as expressed in Equation (1):

$$sk = (L - 1) \sum_{j=0}^{k} \frac{nj}{N} \tag{1}$$

Where sk is the new intensity value, tk is the original intensity value, L is the number of intensity levels, nj is the number of pixels with intensity level j, and N is the total number of pixels.

3.4 LAB Color Space

The CIELAB color space separates lightness information from chromatic information. It consists of three components: L∗, a∗, and b∗. The L∗ component represents lightness, a∗ represents the green-to-red color axis, and b∗ represents the blue-to-yellow color axis. The conversion from RGB to LAB is performed through the XYZ color space. First, the RGB components are normalized and converted to linear RGB values:

$$C_{lin} = \begin{cases} \frac{C}{12.92} \\ \left(\frac{C+0.055}{1.055}\right) \end{cases} 2.4, \begin{matrix} C \le 0.04045 \\ C \ge 0.04045 \end{matrix} \tag{2}$$

Where C represents the normalized R, G, or B component. The linear RGB values are then transformed into the XYZ color space using:

$$\begin{matrix} X \\ Y \\ Z \end{matrix} = \begin{bmatrix} 0.412456 & 40.3575761 & 0.1804375 \\ 0.212672 & 90.7151522 & 0.0721750 \\ 0.019333 & 90.1191920 & 0.9503041 \end{bmatrix} \begin{bmatrix} R \\ G \\ B \end{bmatrix} \tag{3}$$

The XYZ components are normalized using the reference white values:

$$x = \frac{X}{X_n}, \ y = \frac{Y}{Y_n}, \ z = \frac{Z}{Z_n}, \tag{4}$$

Where Xn, Yn, and Zn represent the reference white values. The nonlinear transformation function is defined as:

$$f(t) = \begin{cases} t^{1/3} \\ \frac{1}{3}\left(\frac{29}{6}\right) 2\, t + \frac{4}{29}, \end{cases} \begin{matrix} t > \left(\frac{6}{29}\right) 3 \\ t \le \left(\frac{6}{29}\right) 3 \end{matrix} \tag{5}$$

The LAB components are then calculated as: $L^* = 116\mathrm{f(y)} - 16$, $a^* = 500[\mathrm{f(x)} - \mathrm{f(y)}]$, $b^* = 200[\mathrm{f(y)} - \mathrm{f(z)}]$. The reference white values used in the conversion are: Xn=95.047,Yn=100.000,Zn=108.883.

3.5 HE with LAB

In the HE+LAB configuration, the RGB image is first converted into the LAB color space using the transformation described in the previous subsection. Histogram Equalization is then applied specifically to the L∗ channel. The a∗ and b∗ channels are retained without histogram equalization. The equalization of the L∗ channel is performed using:

$$Leq^* = (Lmax - Lmin) \sum_{j=0}^{k} \frac{nj}{N} + Lmin \tag{6}$$

Where Leq∗ represents the enhanced lightness value, nj represents the number of pixels at intensity level j, and N represents the total number of pixels. The enhanced L∗ channel is then combined with the original a∗ and b∗ channels to form the enhanced LAB image.

3.6 Segmentation Process

The enhanced images are segmented using Otsu thresholding and Canny edge detection. These methods are selected because they represent two different conventional segmentation approaches: intensity-based thresholding and edge-based detection.

1) Otsu Thresholding

Otsu thresholding determines an optimal intensity threshold to separate the image into background and foreground classes. For a threshold t, the probabilities of the two classes are defined as:

$$w_0(t) = \sum_{i=0}^{t} p\ (i) \tag{7}$$

$$w_1(t) = \sum_{i=t+1}^{L-1} p\ (i) \tag{8}$$

Where p(i) represents the normalized histogram of the image and L represents the number of intensity levels. The class means are calculated as:

$$\mu_0(t) = \frac{\sum_{i=0}^{t} i\ p\ (i)}{w_0(t)} \tag{9}$$

$$\mu_0(t) = \frac{\sum_{i=t+1}^{L-1} i\ p\ (i)}{w_1(t)} \tag{10}$$

The optimal threshold is obtained by maximizing the between-class variance:

$$\sigma_B^2(t) = w_0(t)w_1(t)[\mu_0(t) - \ \mu_1(t)\ ]2 \tag{11}$$

The threshold that produces the maximum between-class variance is selected as the optimal Otsu threshold.

2) Canny Edge Detection

Canny edge detection is used to identify intensity boundaries that may correspond to lesion boundaries. The process includes Gaussian smoothing, gradient calculation, non-maximum suppression, and hysteresis thresholding. Gaussian smoothing is expressed as:

$$\mathrm{G}\ (\mathrm{x}, \mathrm{y})\ = \frac{1}{2\pi\sigma^2} e^{\frac{-x^2+y^2}{2\sigma^2}} \tag{12}$$

Where σ represents the standard deviation of the Gaussian filter. The smoothed image is obtained through convolution:

$$\mathrm{Is}(\mathrm{x}, \mathrm{y}) = \mathrm{G}(\mathrm{x}, \mathrm{y}) * \mathrm{I}(\mathrm{x}, \mathrm{y}) \tag{13}$$

Where I(x,y) represents the input image and Is(x,y) represents the smoothed image. The gradient magnitude is calculated as:

$$\mathrm{M}(\mathrm{x}, \mathrm{y}) = \sqrt{G_x^2(x, \mathrm{y}) G_y^2(x, y)} \tag{13}$$

Where Gx and Gy represent the horizontal and vertical image gradients. The gradient direction is calculated using:

$$0(x, y) = tan^{-1} \left(\frac{G_{y\ (x,y)}}{G_{x\ (x,y)}}\right) \tag{14}$$

The resulting edge map is then used as the segmentation output.

3.7 Ground Truth Mask

The ground truth mask is used as the reference for evaluating the segmentation results. In this study, the ground truth mask represents the expert-annotated lesion region in each PH2 image. The lesion region in the ground truth mask is compared pixel by pixel with the segmentation output generated by the Otsu and Canny methods. The ground truth masks are resized according to the corresponding image resolutions of 64 × 64, 128 × 128, and 256 × 256 pixels.

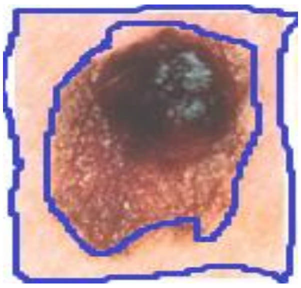

Figure 2. Ground Truth Mask of a Skin Lesion

3.8. Segmentation Evaluation

The segmentation performance is evaluated by comparing the predicted segmentation mask with the corresponding ground truth mask. Five metrics are used: Accuracy, Precision, Recall, F1-Score, and Intersection over Union (IoU). Let TP, TN, FP, and FN represent true positive, true negative, false positive, and false negative pixels, respectively.

$$\text{Accuracy} = \frac{TP+TN}{TP+TN+FN+FP} \tag{15}$$

$$\text{Precision} = \frac{TP}{TP+FN} \tag{16}$$

$$\text{Recall} = \frac{TP}{TP+FP} \tag{17}$$

$$\text{F1} - \text{Score} = 2\,x\,\frac{Precision\ x\ Recall}{Precision + Recall} \tag{18}$$

$$\text{IoU} = \frac{TP}{TP+FN+FP} \tag{19}$$

4. Result and Discussion

4.1 Results

The experiments evaluated the performance of Histogram Equalization (HE) and HE applied to the Lightness (L) channel in the LAB color space (HE+LAB), followed by Canny edge detection and Otsu thresholding. The evaluation was conducted at three image resolutions: 64 × 64, 128 × 128, and 256 × 256 pixels. The resulting segmentation masks were compared with the ground truth masks using Accuracy, Precision, Recall, F1-Score, and Intersection over Union (IoU). The original skin lesion images at resolutions of 64 × 64, 128 × 128, and 256 × 256 pixels were processed using Histogram Equalization (HE). An example of the preprocessing results at a resolution of 128 × 128 pixels is shown in Figure 3.

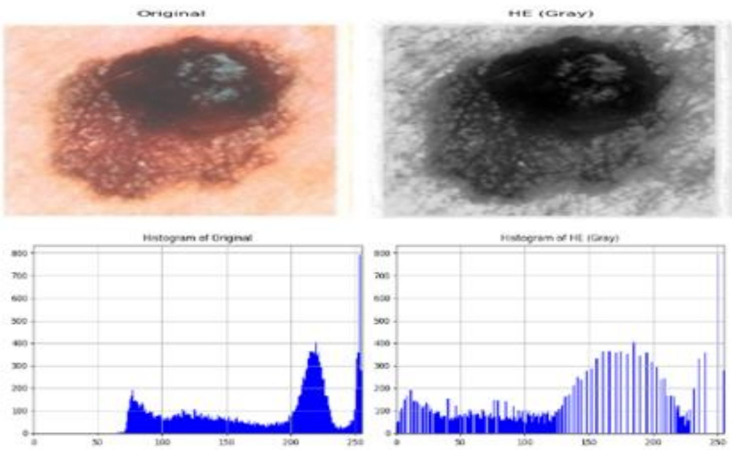

Figure 3. Comparison of skin lesion images at a resolution of 128 × 128 pixels before and after HE preprocessing.

Figure 3 compares the original skin lesion image with the image obtained after grayscale conversion and Histogram Equalization. The original image shows variations in illumination and contrast between the lesion and surrounding skin. These variations may make lesion boundaries difficult to distinguish. After HE processing, the intensity distribution is redistributed over a wider range, resulting in greater contrast between darker and brighter regions. The histograms shown below the images illustrate the change in intensity distribution before and after HE. The histogram of the original image shows a concentration of pixels within particular intensity ranges, whereas the histogram after HE is distributed more broadly across the available intensity range. This indicates that HE changes the global intensity distribution and increases image contrast. After HE preprocessing, segmentation was performed using Canny edge detection and Otsu thresholding. The segmentation results are presented in Figure 4.

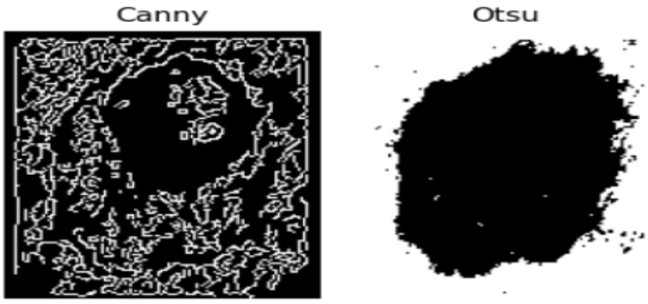

Figure 4. Segmentation results using Canny edge detection and Otsu thresholding after HE preprocessing.

Figure 4 shows that Canny produces edge information along intensity transitions within the image. The resulting edge map contains lesion boundaries as well as other intensity transitions that may originate from skin texture or image artifacts. This characteristic can result in fragmented boundaries and incomplete representation of the lesion region. Otsu thresholding generates a binary segmentation based on an automatically determined global threshold. The resulting regions are more suitable for representing the lesion area because the method assigns pixels to foreground and background classes according to their intensity distribution.

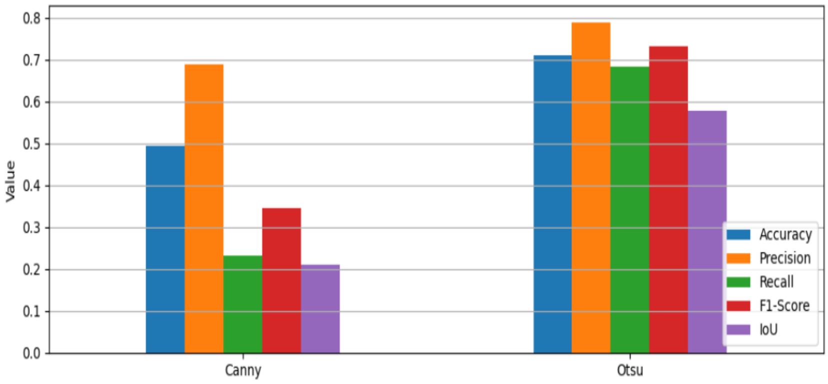

Figure 5. Evaluation results of skin lesion image segmentation after HE preprocessing using Canny edge detection and Otsu thresholding.

Figure 5 presents the quantitative evaluation of the HE-based segmentation results using Canny edge detection and Otsu thresholding. The two methods are compared using Accuracy, Precision, Recall, F1-Score, and Intersection over Union (IoU). The results show that HE-Otsu provides higher values across all evaluation metrics than HE-Canny. In contrast, HE-Canny produces a relatively higher Precision than its Recall, indicating that the method identifies some lesion pixels correctly but does not capture a large proportion of the lesion region.

Table 3. Evaluation results of skin lesion image segmentation at a resolution of 128 × 128 pixels using HE and Canny or Otsu.

Method	Accuracy	Precision	Recall	F1-Score	IoU
HE-Canny	0.4782	0.6889	0.2166	0.3295	0.1973
HE-Otsu	0.7141	0.8103	0.6753	0.7366	0.5831

The HE-Canny method achieves a Precision of 0.6889 but a substantially lower Recall of 0.2166. The resulting F1-Score and IoU are 0.3295 and 0.1973, respectively. These values indicate that the Canny output captures only a limited proportion of the lesion pixels represented in the ground truth mask. The HE-Otsu method produces higher values across all five evaluation metrics. It achieves an Accuracy of 0.7141, Precision of 0.8103, Recall of 0.6753, F1-Score of 0.7366, and IoU of 0.5831. Compared with HE-Canny, these results indicate that Otsu produces a segmentation with greater overlap with the ground truth mask. The second preprocessing configuration applies Histogram Equalization to the L channel of the LAB color space. The comparison of the original and HE+LAB images at a resolution of 128 × 128 pixels is shown in Figure 6.

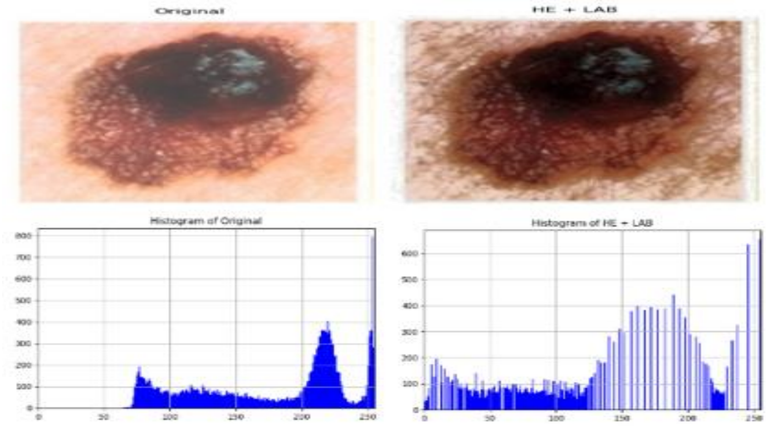

Figure 6. Comparison of skin lesion images at a resolution of 128 × 128 pixels before and after HE+LAB preprocessing.

Figure 6 shows the original image and the image obtained after converting the image to the LAB color space and applying HE to the L channel. The L channel represents lightness, while the a and b channels contain chromatic information. Therefore, the equalization process is applied to the lightness component without directly equalizing the chromatic channels. The HE+LAB result shows a broader lightness distribution than the original image. This change can improve the intensity difference between the lesion and surrounding skin, which may support subsequent threshold-based segmentation. However, HE remains a global contrast enhancement method and may also amplify intensity variations or image artifacts. The segmentation results obtained using Canny and Otsu after HE+LAB preprocessing are shown in Figure 7.

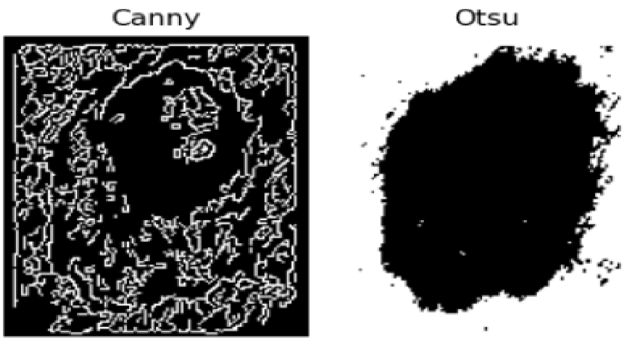

Figure 7. Segmentation results using Canny edge detection and Otsu thresholding after HE+LAB preprocessing.

Figure 7 shows that the Canny method produces numerous edge responses within the image. Some of these edges correspond to lesion boundaries, while others may originate from texture and local intensity variations. As a result, the output may not form a complete lesion region. The Otsu result produces a more continuous binary region. This allows the segmented lesion area to be compared directly with the corresponding ground truth mask using region-based evaluation metrics.

Table 4. Evaluation results of skin lesion image segmentation at a resolution of 128 × 128 pixels using HE+LAB and Canny or Otsu.

Method	Accuracy	Precision	Recall	F1-Score	IoU
HE+LAB-Canny	0.4794	0.6914	0.2180	0.3315	0.1987
HE+LAB-Otsu	0.7170	0.8096	0.6826	0.7407	0.5882

The HE+LAB-Canny method obtains an Accuracy of 0.4794, Precision of 0.6914, Recall of 0.2180, F1-Score of 0.3315, and IoU of 0.1987. Although its Precision is relatively high, the low Recall indicates that a substantial portion of the lesion region is not detected. The HE+LAB-Otsu method achieves higher performance, with an Accuracy of 0.7170, Precision of 0.8096, Recall of 0.6826, F1-Score of 0.7407, and IoU of 0.5882. These results show that HE+LAB combined with Otsu provides better agreement with the ground truth mask than HE+LAB combined with Canny at the 128 × 128 resolution. Tables 5–7 present the segmentation results obtained at 64 × 64, 128 × 128, and 256 × 256 pixels, respectively. The four configurations evaluated were HE-Canny, HE-Otsu, HE+LAB-Canny, and HE+LAB-Otsu.

Table 5. Evaluation results of skin lesion image segmentation at a resolution of 64 × 64 pixels.

Contrast Enhancement - Segmentation	Accuray	Precision	Recall	F1-Score	IoU
HE-Canny	0.4753	0.6597	0.2581	0.3711	0.2278
HE-Otsu	0.7087	0.8106	0.6710	0.7342	0.5801
HE+LAB-Canny	0.4797	0.6667	0.2647	0.3789	0.2337
HE+LAB-Otsu	0.7134	0.8109	0.6808	0.7402	0.5875

At 64 × 64 pixels, HE-Canny obtains the lowest performance, particularly in Recall (0.2581), F1-Score (0.3711), and IoU (0.2278). HE-Otsu achieves higher values, including an F1-Score of 0.7342 and IoU of 0.5801. HE+LAB-Otsu produces slightly higher values, with an Accuracy of 0.7134, F1-Score of 0.7402, and IoU of 0.5875.

Table 6. Evaluation results of skin lesion image segmentation at a resolution of 128 × 128 pixels.

Contrast Enhancement - Segmentation	Accuray	Precision	Recall	F1-Score	IoU
HE-Canny	0.4782	0.6889	0.2166	0.3295	0.1973
HE-Otsu	0.7141	0.8103	0.6753	0.7366	0.5831
HE+LAB-Canny	0.4794	0.6914	0.2180	0.3315	0.1987
HE+LAB-Otsu	0.7170	0.8096	0.6826	0.7407	0.5882

At 128 × 128 pixels, the same pattern is observed. HE+LAB-Otsu achieves an Accuracy of 0.7170, Precision of 0.8096, Recall of 0.6826, F1-Score of 0.7407, and IoU of 0.5882. The Canny-based methods remain substantially lower in Recall, F1-Score, and IoU.

Table 7. Evaluation results of skin lesion image segmentation at a resolution of 256 × 256 pixels.

Contrast Enhancement - Segmentation	Accuray	Precision	Recall	F1-Score	IoU
HE-Canny	0.4486	0.7389	0.1124	0.1951	0.1081
HE-Otsu	0.7150	0.8130	0.6762	0.7383	0.5852
HE+LAB-Canny	0.4482	0.7446	0.1094	0.1907	0.1054
HE+LAB-Otsu	0.7180	0.8127	0.6832	0.7423	0.5903

At 256 × 256 pixels, HE+LAB-Otsu again achieves the highest values among the evaluated configurations at this resolution, with an Accuracy of 0.7180, Precision of 0.8127, Recall of 0.6832, F1-Score of 0.7423, and IoU of 0.5903. These values are slightly higher than those obtained at 128 × 128 pixels.

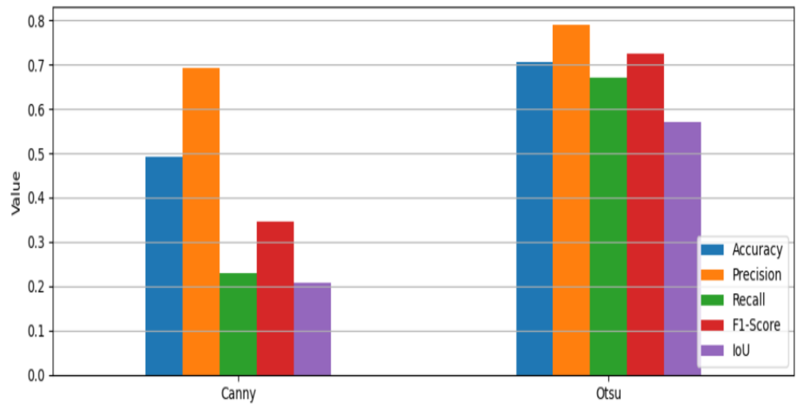

Figure 8. Comparison of segmentation performance across image resolutions and preprocessing configurations.

Figure 8 illustrates the performance trends of the four segmentation configurations across the three evaluated image resolutions. The results show that the HE+LAB-Otsu configuration consistently provides the highest overall segmentation performance, particularly in terms of F1-Score and IoU. The Canny-based configurations show lower performance, especially in Recall and IoU, indicating that edge-based segmentation is less effective in representing the complete lesion region. The Otsu-based configurations show more stable performance across the evaluated resolutions.

4.2 Discussion

The experimental results show that the combination of HE+LAB and Otsu provides the highest segmentation performance among the four evaluated configurations, and this pattern is consistent across the three tested image resolutions. The HE+LAB-Otsu method obtains F1-Scores of 0.7402, 0.7407, and 0.7423 at 64 × 64, 128 × 128, and 256 × 256 pixels, respectively, while the IoU values increase slightly from 0.5875 to 0.5882 and 0.5903. These results indicate that applying HE to the L channel of the LAB color space can provide a useful preprocessing configuration for subsequent Otsu segmentation. Because LAB separates lightness from chromatic components, contrast enhancement can be applied specifically to the L channel without directly equalizing the RGB channels independently. This configuration limits direct modification of chromatic components and may help preserve color-related information. However, the improvement of HE+LAB-Otsu over HE-Otsu remains relatively small, although it is consistent across the tested resolutions.

The comparison between Canny and Otsu shows a clear difference in segmentation behavior. Canny produces edge maps based on intensity gradients and is therefore more focused on boundary detection. In the present experiment, the Canny-based configurations obtain substantially lower Recall, F1-Score, and IoU values than the Otsu-based configurations, suggesting that the detected edges do not represent the complete lesion regions required for region-based comparison with the ground truth masks. Otsu, in contrast, produces a binary region based on an automatically selected global threshold, which makes its output more directly compatible with lesion-region evaluation. At 256 × 256 pixels, for example, HE+LAB-Canny obtains a Recall of only 0.1094 and an IoU of 0.1054. The low Recall indicates that the resulting edge map captures only a small proportion of the lesion pixels represented by the ground truth. This finding supports the observed limitation of using an edge detector directly for region-based skin lesion segmentation, although the present study does not quantify the individual contribution of factors such as hair, illumination, or noise.

The influence of image resolution is relatively limited for the Otsu-based methods. HE+LAB-Otsu obtains its highest values at 256 × 256 pixels, with an Accuracy of 0.7180, F1-Score of 0.7423, and IoU of 0.5903. These values are only slightly higher than those obtained at 128 × 128 pixels. Therefore, the current results do not provide sufficient evidence to conclude that 128 × 128 pixels is the optimal resolution based solely on segmentation performance. A similar pattern is observed in the comparison between HE-Otsu and HE+LAB-Otsu. At 128 × 128 pixels, Accuracy increases from 0.7141 to 0.7170, F1-Score increases from 0.7366 to 0.7407, and IoU increases from 0.5831 to 0.5882. Small improvements are also observed at 64 × 64 and 256 × 256 pixels. These results suggest that LAB-based preprocessing may provide a modest improvement under the experimental conditions used in this study, but statistical testing is required before determining whether these differences are statistically significant.

The proposed approach has several limitations. The evaluation uses only the PH2 Dataset, so the results cannot automatically be generalized to other skin lesion datasets. In addition, the study evaluates conventional image processing methods and does not directly compare them with current deep learning segmentation architectures. The effectiveness of the method may also vary for images with difficult lesion boundaries, strong illumination variations, or other artifacts. Because the study does not report computational time or memory requirements, claims regarding real-time implementation and computational efficiency cannot yet be quantitatively supported. Within these limitations, the results indicate that HE+LAB-Otsu is the best-performing configuration among the methods evaluated in this study. Its performance is consistently higher than that of the other configurations across the three image resolutions, with the highest values obtained at 256 × 256 pixels: Accuracy of 0.7180, Precision of 0.8127, Recall of 0.6832, F1-Score of 0.7423, and IoU of 0.5903. These findings support the use of LAB-based lightness enhancement followed by Otsu thresholding as a conventional approach for skin lesion segmentation under the conditions evaluated in this study.

5. Conclusion and Recommendations

This study concludes that the combination of Histogram Equalization applied to the Lightness (L) channel of the LAB color space (HE+LAB) with Otsu thresholding achieved the best overall segmentation performance among the evaluated methods. Across the three image resolutions, HE+LAB-Otsu consistently produced higher Accuracy, F1-Score, and IoU values than the corresponding Canny-based methods. At a resolution of 128 × 128 pixels, HE+LAB-Otsu achieved an Accuracy of 0.7170, Precision of 0.8096, Recall of 0.6826, F1-Score of 0.7407, and IoU of 0.5882. At 256 × 256 pixels, the method achieved slightly higher values, with an Accuracy of 0.7180, F1-Score of 0.7423, and IoU of 0.5903. These results indicate that HE+LAB provides a useful preprocessing approach for preserving luminance information while maintaining the chromatic components of skin lesion images.

The comparison between segmentation methods shows that Otsu thresholding performs better than Canny edge detection for the evaluated skin lesion images. Canny produced relatively high Precision values but substantially lower Recall, F1-Score, and IoU, indicating that the detected edges did not capture the complete lesion regions. In contrast, Otsu produced more complete region-based segmentation and greater overlap with the ground truth masks. The results across the three resolutions also show that HE+LAB-Otsu maintains relatively consistent performance, while Canny-based methods show a more pronounced decline in Recall and IoU at the 256 × 256 resolution. Overall, the findings indicate that the HE+LAB-Otsu combination is an effective conventional image processing approach for skin lesion segmentation within the PH2 dataset used in this study. However, the results should not be interpreted as evidence of clinical readiness because the study was limited to a single dataset and did not include external validation or clinical evaluation.

Future research should evaluate the proposed approach using additional skin lesion datasets to determine its generalizability across different image acquisition conditions and lesion characteristics. Further studies may also investigate morphological filtering or other post-processing techniques to reduce small artifacts and improve lesion boundaries after Otsu segmentation. In addition, the HE+LAB preprocessing approach can be evaluated as an input preprocessing stage for deep learning segmentation architectures such as U-Net. Comparisons with modern segmentation models and statistical significance testing are also recommended to determine whether the observed performance differences are statistically meaningful. Computational measurements such as processing time and memory usage should also be included if computational efficiency is intended to be a major consideration.

References

Agrawal, H., & Desai, K. (2024). Canny edge detection: A comprehensive review. *International Journal of Technical Research & Science, 1*(1), 7.

Al-Hatab, M. M. M., Ibrahim Al-Obaidi, A. S., & Al-Hashim, M. A. (2024). Exploring CIE Lab color characteristics for skin lesion images detection: A novel image analysis methodology incorporating color-based segmentation and luminosity analysis. *Fusion: Practice and Applications, 15*(1), 88–97. https://doi.org/10.54216/FPA.150108

Basha, S. M., Chandrika, K. N., Sravani, K., Sandeep, M., & Abhiram, G. (2025). *Enhanced lane detection using Otsu-Canny edge detection and Hough transform*. Zenodo. https://doi.org/10.5281/zenodo.15084883

Ding, C., Pan, X., Gao, X., Ning, L., & Wu, Z. (2020). Three adaptive sub-histograms equalization algorithm for maritime image enhancement. *IEEE Access, 8*, 147983–147994. https://doi.org/10.1109/ACCESS.2020.3015839

Ebele, O., Doris, A., & Joy, O. (2025). Exploring the effectiveness of Sobel, Canny, and Prewitt edge detection algorithms on digital images. *World Journal of Advanced Engineering Technology and Sciences, 15*(1). https://doi.org/10.30574/wjaets.2025.15.1.0346

Fawzi, A., Achuthan, A., & Belaton, B. (2021). Adaptive clip limit tile size histogram equalization for non-homogenized intensity images. *IEEE Access, 9*, 164466–164492. https://doi.org/10.1109/ACCESS.2021.3134170

Hadiq, H., Solehatin, S., Djuniharto, D., Muslim, M. A., & Salahudin, S. N. (2023). Comparison of the suitability of the Otsu method thresholding and multilevel thresholding for flower image segmentation. *Journal of Soft Computing Exploration, 4*(4), 242–249. https://doi.org/10.52465/joscex.v4i4.266

I Made Satria Bimantara, & Yuniarti, A. (2023). Multilevel thresholding of color image segmentation using memory-based grey wolf optimizer with Otsu method, Kapur, and M. Masi entropy. *Jurnal Nasional Pendidikan Teknik Informatika (JANAPATI), 12*(2), 304–337. https://doi.org/10.23887/janapati.v12i2.62874

Jabber, A. A., Shadeed, G. A., Salim, N., & Dibs, H. (2025). Automated skin lesion diagnosis and classification using K-mean, LAB-color-space segmentation and deep learning. *Operations Research Forum, 6*(2). https://doi.org/10.1007/s43069-025-00430-3

Jawad, E. M., Daway, H. G., & Mohamad, H. J. (2022). Retinal image enhancement by using adapted histogram equalization based on segmentation and Lab color space. *International Journal of Intelligent Engineering and Systems, 15*(3), 614–622. https://doi.org/10.22266/ijies2022.0630.52

Jing, Z., & Tang, B. (2024). Improved image segmentation method based on Otsu thresholding and level set techniques. *Journal of Physics: Conference Series, 2813*(1), 012017. https://doi.org/10.1088/1742-6596/2813/1/012017

Karakus, P. (2025). Detection of water surface using Canny and Otsu threshold methods with machine learning algorithms on Google Earth Engine: A case study of Lake Van. *Applied Sciences, 15*(6). https://doi.org/10.3390/app15062903

Katherine, Rulaningtyas, R., & Ain, K. (2021). CT scan image segmentation based on Hounsfield unit values using Otsu thresholding method. *Journal of Physics: Conference Series, 1816*(1), 012080. https://doi.org/10.1088/1742-6596/1816/1/012080

Liu, Y., Qiu, G., & Wang, N. (2024). A novel method for peanut seed plumpness detection in soft X-ray images based on level set and multi-threshold OTSU segmentation. *Agriculture, 14*(5). https://doi.org/10.3390/agriculture14050765

Manikandan, S. P., Narani, S. R., Karthikeyan, S., & Mohankumar, N. (2025). Deep learning for skin melanoma classification using dermoscopic images in different color spaces. *International Journal of Electrical and Computer Engineering, 15*(1), 319–327. https://doi.org/10.11591/ijece.v15i1.pp319-327

Ng, Y. J., & Sim, K. S. (2024). A review of brain early infarct image contrast enhancement using various histogram equalization techniques. *International Journal on Advanced Science, Engineering and Information Technology, 14*(6), 1849–1860. https://doi.org/10.18517/ijaseit.14.6.10115

Rahmawati, A., Yulianti, I., & Nurajizah, S. (2023). Image segmentation analysis using Otsu thresholding and. *Jurnal Riset Informatika, 6*(1).

Saifullah, S., Drezewski, R., Khaliduzzaman, A., Tolentino, L. K., & Ilyos, R. (2022). K-means segmentation based on Lab color space for embryo detection in incubated egg. *Jurnal Ilmiah Teknik Elektro Komputer dan Informatika, 8*(2), 175. https://doi.org/10.26555/jiteki.v8i2.23724

Saifullah, S., Suryotomo, A. P., Dreżewski, R., Tanone, R., & Tundo, T. (2024). Optimizing brain tumor segmentation through CNN U-Net with CLAHE-HE image enhancement. In *Proceedings of the 2023 1st International Conference on Advanced Informatics and Intelligent Information Systems (ICAI3S 2023)* (pp. 90–101). https://doi.org/10.2991/978-94-6463-366-5_9

Setty, A. N., Mathad, R. T., Shenthar, K., & Likhith. (2024). Evaluation of filtering and contrast in X-ray and computerized tomography scan lung classification. *Indonesian Journal of Electrical Engineering and Computer Science, 33*(3), 1715–1725. https://doi.org/10.11591/ijeecs.v33.i3.pp1715-1725

Surmayanti, S., & Sumijan, S. (2024). Improving digital image clarity: A study on the application of histogram equalization for noise correction. *Sinkron, 8*(2), 1073–1079. https://doi.org/10.33395/sinkron.v8i2.13564

Syafi'i, R., & Khomsah, S. (2024). Classification of Indonesian batik: A comparative study of CNN and VGG16 with Canny edge detection. In *COMNETSAT 2024—IEEE International Conference on Communication, Networks and Satellite* (pp. 355–363). https://doi.org/10.1109/COMNETSAT63286.2024.10862216

Thanh, D. N. H., Erkan, U., Surya Prasath, V. B., Kumar, V., & Hien, N. N. (2019). A skin lesion segmentation method for dermoscopic images based on adaptive thresholding with normalization of color models. In *Proceedings of the 2019 6th International Conference on Electrical and Electronics Engineering (ICEEE 2019)* (pp. 116–120). https://doi.org/10.1109/ICEEE2019.2019.00030

Tundo, Saifullah, S., Yel, M. B., Irawansah, O., Mubarak, Z. Y., & Saidah, A. (2024). Prediction of palm oil production using hybrid decision tree based on fuzzy inference system Tsukamoto. *Bulletin of Electrical Engineering and Informatics, 13*(6), 4182–4192. https://doi.org/10.11591/eei.v13i6.7773

Zare, H., Ramezanzadeh, E., Shoeibi, N., & Shariati, M. M. (2024). A high-accuracy segmentation hybrid method for retinal blood vessel detection in fluorescein angiography images of real diabetic retinopathy patients. https://doi.org/10.1364/opticaopen.25465552.v1